Journal of Zhejiang University-SCIENCE B (Biomedicine & Biotechnology) *2024 25(1):51-64*
www.jzus.zju.edu.cn; www.springer.com/journal/11585
E-mail: jzus_b@zju.edu.cn

Research Article

https://doi.org/10.1631/jzus.B2200652

Mass spectrometry analysis of intact protein *N*-glycosylation signatures of cells and sera in pancreatic adenocarcinomas

Mingming XU[1], Zhaoliang LIU[1], Wenhua HU[1], Ying HAN[2], Zhen WU[3], Sufeng CHEN[4], Peng XIA[4], Jing DU[4], Xumin ZHANG[3], Piliang HAO[2], Jun XIA[4]✉, Shuang YANG[1]✉

[1]*Center for Clinical Mass Spectrometry, College of Pharmaceutical Sciences, Soochow University, Suzhou 215123, China*
[2]*School of Life Science and Technology, ShanghaiTech University, Shanghai 201210, China*
[3]*State Key Laboratory of Genetic Engineering, Department of Biochemistry, School of Life Sciences, Fudan University, Shanghai 200438, China*
[4]*Department of Clinical Laboratory Center, Zhejiang Provincial People's Hospital, People's Hospital of Hangzhou Medical College, Hangzhou 310014, China*

Abstract: Pancreatic cancer is among the most malignant cancers, and thus early intervention is the key to better survival outcomes. However, no methods have been derived that can reliably identify early precursors of development into malignancy. Therefore, it is urgent to discover early molecular changes during pancreatic tumorigenesis. As aberrant glycosylation is closely associated with cancer progression, numerous efforts have been made to mine glycosylation changes as biomarkers for diagnosis; however, detailed glycoproteomic information, especially site-specific *N*-glycosylation changes in pancreatic cancer with and without drug treatment, needs to be further explored. Herein, we used comprehensive solid-phase chemoenzymatic glycoproteomics to analyze glycans, glycosites, and intact glycopeptides in pancreatic cancer cells and patient sera. The profiling of *N*-glycans in cancer cells revealed an increase in the secreted glycoproteins from the primary tumor of MIA PaCa-2 cells, whereas human sera, which contain many secreted glycoproteins, had significant changes of glycans at their specific glycosites. These results indicated the potential role for tumor-specific glycosylation as disease biomarkers. We also found that AMG-510, a small molecule inhibitor against Kirsten rat sarcoma viral oncogene homolog (*KRAS*) G12C mutation, profoundly reduced the glycosylation level in MIA PaCa-2 cells, suggesting that *KRAS* plays a role in the cellular glycosylation process, and thus glycosylation inhibition contributes to the anti-tumor effect of AMG-510.

Key words: Pancreatic cancer; Glycosylation; Biomarker; Glycoproteomics; Mass spectrometry

1 Introduction

As one of the most lethal cancers, pancreatic cancer (PC) was responsible for approximately 500 000 new cases and more than 450 000 deaths worldwide in 2020 (Sung et al., 2021). More than 90% of PC cases are pancreatic ductal adenocarcinoma (PDAC). Due to the limitations of current diagnostic methods, 80%–85% of PDAC patients are diagnosed at an advanced stage, and the 5-year survival rate is less than 5% (Ryan et al., 2014). Sporadic PDAC accounts for 90% of all cases and usually involves mutations in the oncogene Kirsten rat sarcoma viral oncogene homolog (*KRAS*) and tumor suppressor genes cyclin-dependent kinase inhibitor 2A (*CDKN2A*), tumor protein p53 (*TP53*), and mothers against decapentaplegic homolog 4 (*SMAD4*) (Hruban et al., 1998). PDAC driver genes are intimately involved in various signaling pathways leading to carcinogenesis (Hu et al., 2021). Of note, many proteins that regulate PDAC signaling pathways are modified by glycosylation, which is one of the most common post-translational modifications. For instance, *KRAS* expresses Le^x that is a Lewis antigen (Rho et al., 2014). Other proteins, including epithelial growth factor receptor (EGFR) (Ardito et al., 2012), transforming growth factor-β receptor (TGFβR) (Pan et al., 2012), and integrin

✉ Shuang YANG, yangs2020@suda.edu.cn
Jun XIA, andisky_005@126.com
Shuang YANG, https://orcid.org/0000-0001-7958-0594
Jun XIA, https://orcid.org/0000-0003-3222-2882

Received Dec. 18, 2022; Revision accepted May 12, 2023; Crosschecked Dec. 21, 2023

(Bassagañas et al., 2014), are post-translationally modified by various glycans. Aberrant glycosylation has been observed in PDAC tumor progression. For example, PC cells often have increased levels of highly branched *N*-glycans, sialylated or fucosylated complex *N*-glycans (Munkley, 2019). In fact, glycosylation has multiple functions and contributes to the hallmarks of PDAC as an active regulator of disease onset, tumor progression, metastatic capability, therapeutic resistance, and remodeling the tumor immune microenvironment (Lumibao et al., 2022). Thus, the identification of PDAC-specific glycosylation changes is key to discovering potential biomarkers for early diagnosis (Xu et al., 2021; Yang et al., 2021).

Mass spectrometry (MS) has been widely used to quantitatively characterize glycosylation in complex biological samples (Xiao et al., 2019). Vreeker et al. (2020) found that a total of 23 different *N*-glycans were associated with PDAC, including branching, fucosylation, and sialylation traits. These signatures were also observed in PDAC sera. PDAC-specific changes in glycosylation may be due to the differential expression of glycosyltransferases that define PDAC glycosylation traits (Abd-El-Halim et al., 2021). The serum *N*-glycome of individuals at risk for PDAC also showed the significant upregulation of fucosylation, tri- and tetra-antennary structures, as well as specific sialic linkages (Levink et al., 2022). *N*-Glycomic profiling has also been conducted in PDAC cell lines by matrix-assisted laser desorption/ionization (MALDI)-MS (Park et al., 2015). Increased levels of high-mannose *N*-glycans were found in metastasized Capan-1 cells, whereas highly-branched sialylated *N*-glycans were more abundant in primary tumor cells of Panc-1 and MIA PaCa-2, indicating the role of glycosylation in PDAC metastasis and biomarker discovery.

Site-specific analysis is a common technique to identify disease-specific glycosylation. Glycomic analysis measures the overall change of glycans without considering the protein substrates, and thereby information about the changes of glycosites and site-specific glycan profiling is lost. There are also quantitative analyses of deglycosylated peptides in PDAC sera (Nie et al., 2014) and intact glycopeptides in PDAC tissues (Lu et al., 2021). Intact *N*-glycoproteomics found that immunoglobulin G1 (IgG1) N180 expression was significantly decreased in PDAC patient sera compared to healthy controls (Ctrl) (Liu et al., 2021). Using multiple *N*-glycosidases, 782 core fucosylated glycosites have been associated with PDAC tissue (Cao et al., 2022), but the correlation between PDAC cells and clinical sera in terms of *N*-glycoproteomic changes has not been investigated. In addition, how glycosylation in PDAC cells is altered by inhibiting oncogene functions has not been studied.

In the present study, we used a comprehensive approach involving MS analysis to elucidate detailed *N*-glycosylation changes in PDAC cell lines and sera (Fig. 1). First, we studied *N*-glycan profiles in PDAC cell lines and used *KRAS* G12C-targeted AMG-510 to treat primary cancer cells. The *N*-glycans from secreted glycoproteins in cell culture media were also analyzed. Then, deglycopeptides and intact glycopeptides from cell lines and human sera were assessed by liquid chromatography-tandem MS (LC-MS/MS). The above workflow was previously applied to evaluate the comprehensive serum *N*-glycosylation changes in Parkinson's disease (Xu et al., 2022), and the results showed that site-specific glycosylation changes can provide a more detailed trait for biomarker discovery than the overall glycan profile.

2 Materials and methods

2.1 Enrichment of *N*-glycan

N-Glycans were enriched by a solid-phase chemoenzymatic method (Yang et al., 2013, 2017). Briefly, serum (10 μL) was first denatured at 90 °C for 10 min and mixed with 200 μL of AminoLink plus resin (Thermo Fisher Scientific, USA) in a spin column (Beyotime, China). Proteins were conjugated to the resin in 1× binding buffer (10 mmol/L sodium citrate and 5 mmol/L Na_2CO_3) for 4 h at room temperature (RT), followed by 50 mmol/L $NaCNBH_3$ (Sigma-Aldrich, USA). The resin was washed with 1× phosphate-buffered saline (PBS) and the sample was further incubated for 4 h in 1× PBS containing 50 mmol/L $NaCNBH_3$. After blocking the unreacted resin with 1 mol/L Tris-HCl (pH=7.4), the sialic acids were derivatized with 0.25 mol/L *N*-(3-(dimethylaminopropyl)-*N*'-ethylcarbodiimide (EDC) (Meryer, China)/0.25 mol/L 1-hydroxybenzotriazole (HOBt) hydrate (Sigma-Aldrich) in ethanol at 37 °C for 1 h and then labelled with 1 mol/L *p*-toluidine (pT) (TCI, Japan). The resin

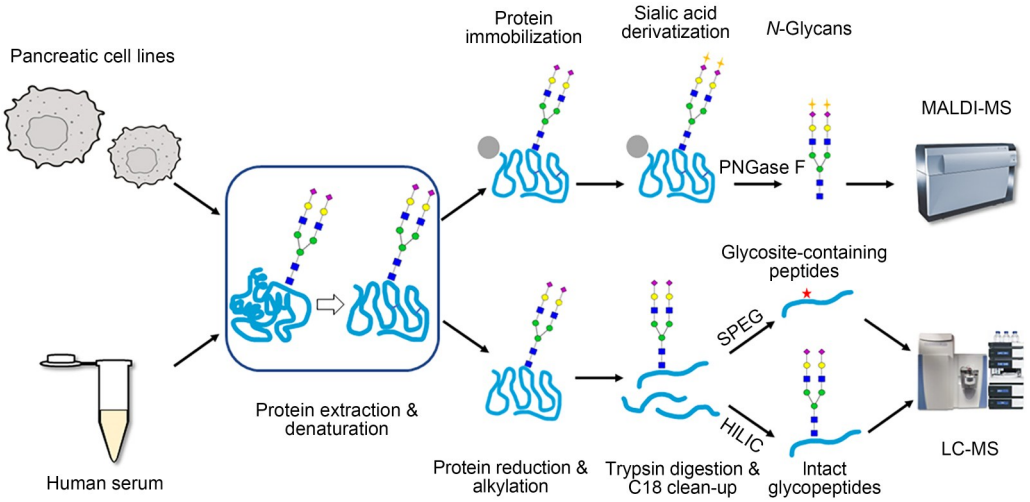

Fig. 1 Workflow of the combined mass spectrometry (MS)-platform for the analysis of glycans, glycosite-containing peptides, and intact glycopeptides in pancreatic cell lines and serum samples. The proteins extracted from cell lines and serum are denatured. For *N*-glycan analysis, proteins are first immobilized and then sialic acid residues of glycoproteins are protected by a two-step derivatization. *N*-Glycans released by peptide-*N*-glycosidase F (PNGase F) are analyzed by matrix-assisted laser desorption/ionization-MS (MALDI-MS). For intact *N*-glycopeptide analysis, proteins are first reduced and alkylated, and subsequently digested by trypsin. After C18 clean-up, glycosite-containing peptides are enriched by solid-phase extraction of N-linked glycopeptide (SPEG) enrichment, and intact glycopeptides are enriched by hydrophilic interaction liquid chromatography (HILIC). Peptide analysis is conducted by liquid chromatography (LC)-MS.

was then washed with 500 μL of 10% (volume fraction) formic acid (Sinopharm Chemical, China), 500 μL of 10% (volume fraction) acetonitrile (ACN) (Tedia, USA), 500 μL of 1 mol/L NaCl (Sinopharm Chemical), and deionized water (all for three times). *N*-Glycans were cleaved from the immobilized glycoproteins by peptide-*N*-glycosidase F (PNGase F) (New England Biolabs, USA) prepared in 25 mmol/L NH_4HCO_3, at 37 ℃ for at least 2 h or overnight. The enriched *N*-glycans were dried in a vacuum concentrator (Jiaimu, China).

2.2 Enrichment of *N*-glycosite-containing peptides

Serum (60 μL) was dissolved in 190 μL 8 mol/L urea (Aladdin, China) prepared in 1 mol/L NH_4HCO_3 and mixed with 25 μL 120 mmol/L tris-(2-carboxyethyl) phosphine hydrochloride (TCEP) (Macklin, China) at 37 ℃ for 1 h. Protein alkylation was then conducted by adding 27.5 μL 160 mmol/L iodoacetamide (IAA) (Aladdin) at RT for 1 h in the dark. The alkylated samples were diluted 5-fold with high-performance liquid chromatography (HPLC)-grade water (J&K, China) and digested by adding 40 μg sequencing grade trypsin (Promega, USA) at 37 ℃ overnight. The digested samples were mixed with 10% formic acid for pH adjustment (<3) and further purified by C18 solid-phase extraction (SPE). Peptides containing *N*-glycosites were enriched by the SPE of N-linked glycopeptides (SPEG) (Zhang et al., 2003). Briefly, C18-purified peptides were oxidized in the dark by 10 mmol/L sodium periodate (Macklin). After C18 clean-up, the glycopeptides were mixed with 1% (volume fraction) aniline (Aladdin) and coupled to hydrazide resin (Thermo Fisher Scientific). The resin was washed with 1.5 mol/L NaCl, deionized water, and 25 mmol/L NH_4HCO_3, and the glycosite-containing peptides were released by PNGase F (prepared in 25 mmol/L NH_4HCO_3). The enriched peptides were dried in a vacuum concentrator.

2.3 Enrichment of intact glycopeptides

C18-purified peptides after trypsin digestion in the previous section were dissolved in 80% ACN with 0.1% (volume fraction) trifluoroacetic acid (TFA) (Macklin). Subsequently, samples were loaded onto the hydrophilic interaction liquid chromatographic (HILIC) column containing Amide-80 gel slurry (Tosoh, Japan), and the flow-through was collected and reloaded. The HILIC column was washed with 80% ACN in 0.1% TFA for three times and eluted with 60% ACN in

0.1% TFA, 40% ACN in 0.1% TFA, and 0.1% TFA (Yang et al., 2018). The eluate was dried in a vacuum concentrator.

2.4 MS analysis of *N*-glycans and *N*-glycopeptides

A Bruker ultrafleXtreme MALDI-MS instrument was employed for the analysis of glycans. Details about sample processing before MS analysis can be found in a previous study (Xu et al., 2022). The positive reflector mode was applied when obtaining all spectra, with a mass range of 900–4000. The laser power was set as 50% and a total of 1000 shots were accumulated for each spectrum in MS mode. Each group contained four replicates. The signal-to-noise (s/n) was set as ≥2 for creating the glycan peak list in the Bruker flexAnalysis software. By searching the databases in the GlycoWorkbench software (Ceroni et al., 2008), the glycan composition was determined.

The glycosite-containing peptides and intact glycopeptides were analyzed by a Q Exactive HF-X Hybrid Quadrupole-Orbitrap Mass Spectrometer (Thermo Fisher Scientific) coupled with an Easy-nLC 1200 system. The detailed procedures and parameters for the MS analysis of peptides are described in previous studies (Yang et al., 2018; Xu et al., 2022). The glycosite-containing peptides enriched in the SPEG experiment were analyzed by the Proteome Discoverer software (Thermo Fisher Scientific) to provide the accession numbers of all identified *N*-glycoproteins. The glycopeptide databases of PDAC sera and cell lines were established by importing the accession numbers into GlycReSoft software (Maxwell et al., 2012), and glycopeptide search spaces were built by assigning biosynthetically feasible human *N*-glycans to the sequences of all identified *N*-glycoproteins. The LC-MS/MS data were analyzed by matching the glycopeptide search space against the MS^2 fragments. The false-discovery rate (FDR) was set at 1%.

3 Results

3.1 *N*-Glycosylation changes in pancreatic cell lines

We first analyzed *N*-glycans from three pancreatic cell lines, including normal hTERT-HPNE, primary pancreatic tumor MIA PaCa-2, and metastatic pancreatic tumor AsPC-1. These cells can be used to mimic oncogenic process to discover PDAC-related changes in glycosylation. The MALDI-MS analysis of *N*-glycans from pancreatic cells identified 30 *N*-glycans (s/n≥2) in hTERT-HPNE cells, including high-mannose and galactosylated, fucosylated and/or sialylated structures (Fig. 2a). Consistent with the study by Holst et al. (2017), the major *N*-glycan peaks in hTERT-HPNE cells were high-mannose, which can be further enzymatically processed into complex or hybrid *N*-glycans. However, in MIA PaCa-2 cells, contrasting changes in the *N*-glycan peak pattern were revealed compared with hTERT-HPNE cells, as shown in Fig. 2b. In the mass-to-charge ratio (m/z) range between 1200 and 2000 units, only five high-mannose *N*-glycans (Man5, Man6, Man7, Man8, and Man9) were clearly observed in the MALDI-MS spectrum. Meanwhile, new *N*-glycan structures, including bisecting and tetra-antennary fucosylated *N*-glycans, were identified in the m/z range between 2000 and 3100 units (Fig. 2b). Interestingly, the *N*-glycan peak pattern of AsPC-1 cells did not show striking changes compared with hTERT-HPNE cells. Instead, the peak patterns of AsPC-1 and hTERT-HPNE cells shared similarity (Fig. 2c). A probable explanation is that PDAC-associated abnormal glycosylation occurs at *N*-glycosites, rather than the overall changes in *N*-glycans (Pan et al., 2014).

An internal standard maltoheptaose (DP7), whose intensity was set to 100%, was used to quantify *N*-glycan changes in pancreatic cell lines (Figs. 2d–2g). High-mannose glycans (Man6, Man7, and Man8) were significantly increased in MIA PaCa-2 compared to hTERT-HPNE, suggesting enhanced cellular glycosylation in the primary tumor cell line. Elevated levels of high-mannose *N*-glycans were also found in various cancer types (de Leoz et al., 2011; Sethi et al., 2016; Chen et al., 2017). Except for a few fucosylated and sialylated structures (H4N5F1, H5N5F1, H6N6F1, S(6)1H5N4F1, and S(6)1H6N5F1), most other *N*-glycans in MIA PaCa-2 were significantly decreased (Figs. 2d–2g, Table S1). Given the enhanced cellular glycosylation in MIA PaCa-2, the reduced levels of galactosylated, fucosylated and/or sialylated *N*-glycans may be attributed to the secretion of *N*-glycoproteins into the extracellular media. To confirm the increase in the secreted *N*-glycoproteins from MIA PaCa-2, the supernatant of the culture media was collected and concentrated. *N*-Glycans from cell culture media were enriched and analyzed by MALDI-MS. In accord with

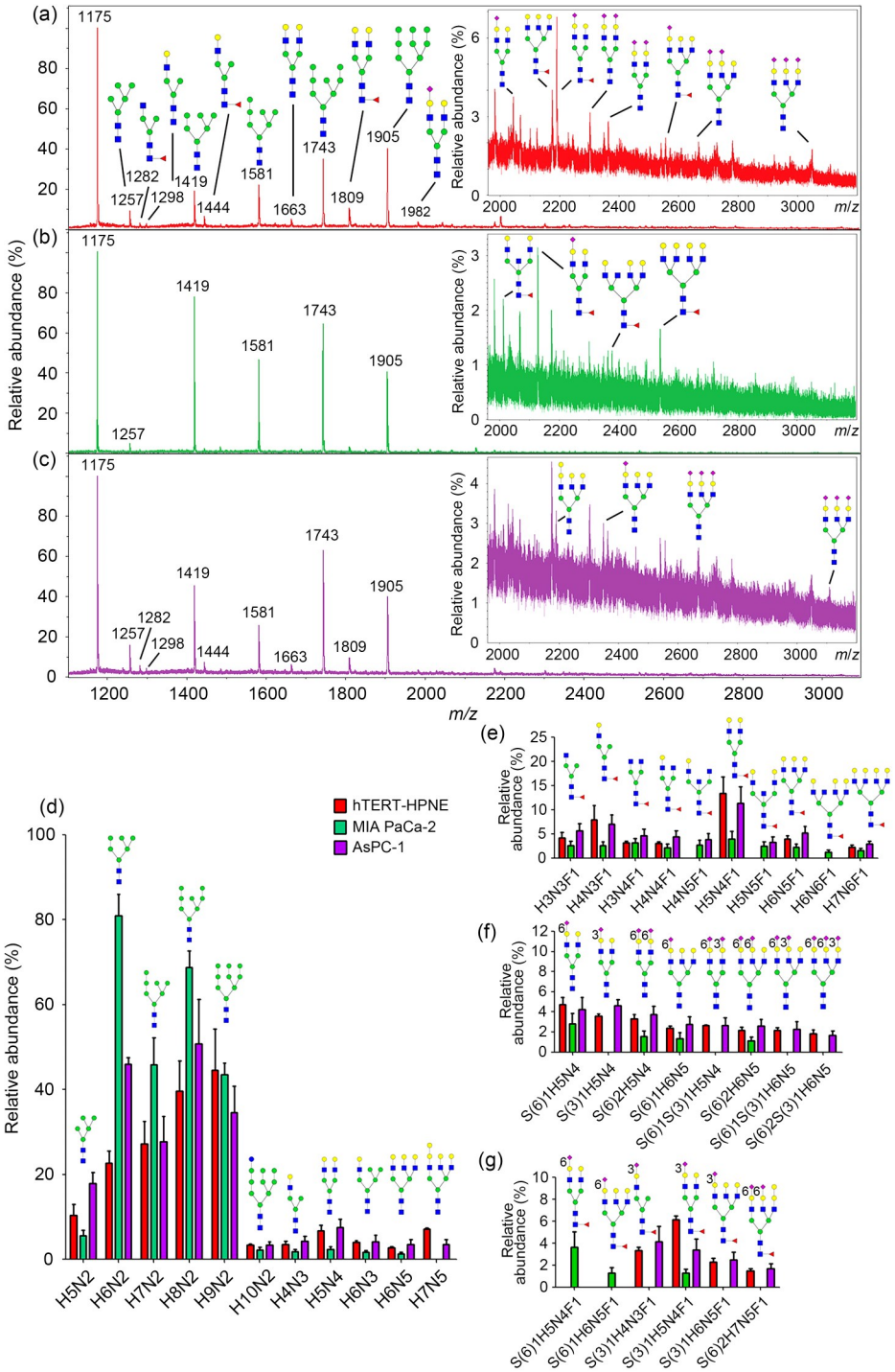

Fig. 2 Matrix-assisted laser desorption/ionization-mass spectrometry (MALDI-MS) spectra of *N*-glycans from pancreatic cell lines, and the quantitative analysis of different types of *N*-glycans. (a) Normal pancreatic cell lines hTERT-HPNE; (b) Primary pancreatic tumor MIA PaCa-2; (c) Metastatic pancreatic tumor AsPC-1; (d) High-mannose and galactosylated *N*-glycans; (e) Fucosylated *N*-glycans; (f) Sialylated *N*-glycans; (g) Fucosylated and sialylated *N*-glycans. (The numbers above the peaks represent the corresponding mass-to-charge ratio (*m*/*z*) values. The peak at 1175 represents the internal standard maltoheptaose (DP7). As seen in the upper right corner of the spectrum, the magnified spectrum is in the *m*/*z* range between 2000 and 3100. The different saccharide units are denoted by colored shapes (red triangle, fucose; green circle, mannose; yellow circle, galactose; blue square, *N*-acetyl glucosamine; purple diamond, sialic acid). The monosaccharide units of all *N*-glycans are represented by capital initials (F: fucose; H: hexose, including glucose, galactose, and mannose; N: *N*-acetyl hexosamine; S(6): α2,6-linked sialic acid; S(3): α2,3-linked sialic acid) (Note: for interpretation of the references to color in this figure legend, the reader is referred to the web version of this article). The same below).

our expectations, many decreased *N*-glycans (H4N3F1, H4N4F1, H5N4, H5N4F1, S(6)1H5N4, H6N5, H6N5F1, S(6)2H5N4, H7N6F1, and S(6)2H6N5) in MIA PaCa-2 cells were observed in the culture media (Fig. S1), which confirms the hypothesis of enhanced intracellular glycosylation activity and extracellular secretion of glycoproteins in primary tumor cell lines (Munkley, 2019). Nevertheless, statistical analysis revealed that in metastatic AsPC-1 cells, glycosylation was restored to a level similar to that of hTERT-HPNE (Figs. 2d–2g, Table S1), indicating a potential feedback regulation of glycosylation in the metastatic stage of PDAC carcinogenesis (Reily et al., 2019). This phenomenon highlights the clinical application value of targeting glycosylation changes in primary tumors to achieve the early diagnosis and treatment of PDAC.

3.2 Effect of AMG-510 on MIA PaCa-2 cells with *KRAS* G12C mutation

Sotorasib (AMG-510) is currently the only US Food and Drug Administration (FDA)-approved small molecule inhibitor that targets solid tumors with the *KRAS* G12C mutation. It has been found to potently impair cellular viability in MIA PaCa-2 (with *KRAS* G12C mutation), while non-*KRAS* G12C cell lines were insensitive to the treatment (Canon et al., 2019). Considering the involvement of aberrant glycosylation in PDAC carcinogenesis, we were eager to investigate whether AMG-510 treatment affects cellular glycosylation levels. The protein concentrations in treated and untreated cells after lysis were determined by bicinchoninic acid (BCA) assay, and equal amounts of proteins were loaded to enrich for *N*-glycans. The MALDI-MS spectra revealed that the intensity of all observable *N*-glycans was reduced notably after AMG-510 treatment (1 and 10 μmol/L) for 24 h (Figs. 3a–3c). Statistical analysis further demonstrated that the inhibition of *N*-glycosylation was non-selective and that the effect of AMG-510 was dose-dependent for most *N*-glycans (Figs. 3d–3f, Table S2). Under the same conditions in our experiments, treatment with AMG-510 (1 and 10 μmol/L) for 24 h only slightly reduced the cell viability of MIA PaCa-2 in the cell counting kit-8 (CCK-8) assay, indicating that AMG-510 treatment was the main contributor to the significant reduction in *N*-glycosylation in MIA PaCa-2 (Fig. S2). *KRAS* mutation was found to drive glycolytic flux in lung cancer and ultimately impact aberrant protein glycosylation (Taparra et al., 2018). The general inhibition of *N*-glycosylation by AMG-510 suggested that this drug can affect the initial stage of *N*-glycan biosynthesis (synthesis of high-mannose structures) by covalently binding to *KRAS* G12C or other off-target pathways. Our results uncovered the effect of AMG-510 on cellular *N*-glycosylation and added new knowledge to the understanding of the antitumor mechanism of AMG-510. Nonetheless, further studies are still needed to establish a detailed connection between AMG-510 and glycosylation biosynthesis.

3.3 *N*-Glycosylation changes in pancreatic patient sera

In clinical practice, the early diagnosis and treatment monitoring of PDAC can be conveniently accomplished through blood tests. CA19-9, a carbohydrate-associated antigen, is an FDA-approved PDAC glycosylation biomarker that primarily evaluates responses to PDAC therapy. Although the CA19-9 blood test can support diagnosis, it fails to provide a definitive conclusion due to its low specificity (Gold et al., 2019). The elevated serum CA19-9 is not specific to PDAC and can also be upregulated in other cancers, including colorectal carcinoma (Vukobrat-Bijedic et al., 2013), gastric cancer (Liang et al., 2016), and lung adenocarcinoma (Sato et al., 2016). Non-cancer diseases also exhibit increased blood levels of CA19-9, such as jaundice (Marrelli et al., 2009), liver inflammation (Zhang et al., 2021), and pancreatitis (Talar-Wojnarowska et al., 2011). As a result, identifying PDAC-specific glycosylation changes is a priority in the development of diagnostic biomarkers. To this end, the overall *N*-glycans in human serum samples from Ctrl, untreated PDAC patients (PDAC), PDAC patients treated with surgery and chemotherapy (PDAC-T), and untreated PDAC patients with additional diseases (PDAC-D) were analyzed. The information of all PDAC patients was listed in Table S3. Unlike the pancreatic cell lines, the major *N*-glycans in human sera carry fucoses and sialic acids in the MALDI-MS spectra (Figs. 4a–4d). A certain variation in the *N*-glycan peak patterns was observed in the four groups. Statistical analysis revealed that only five *N*-glycans (H11N2, H3N4F1, S(6)1H5N4, S(3)1H4N5F2, and S(3)1H6N3F2) were significantly increased in the PDAC group compared with the

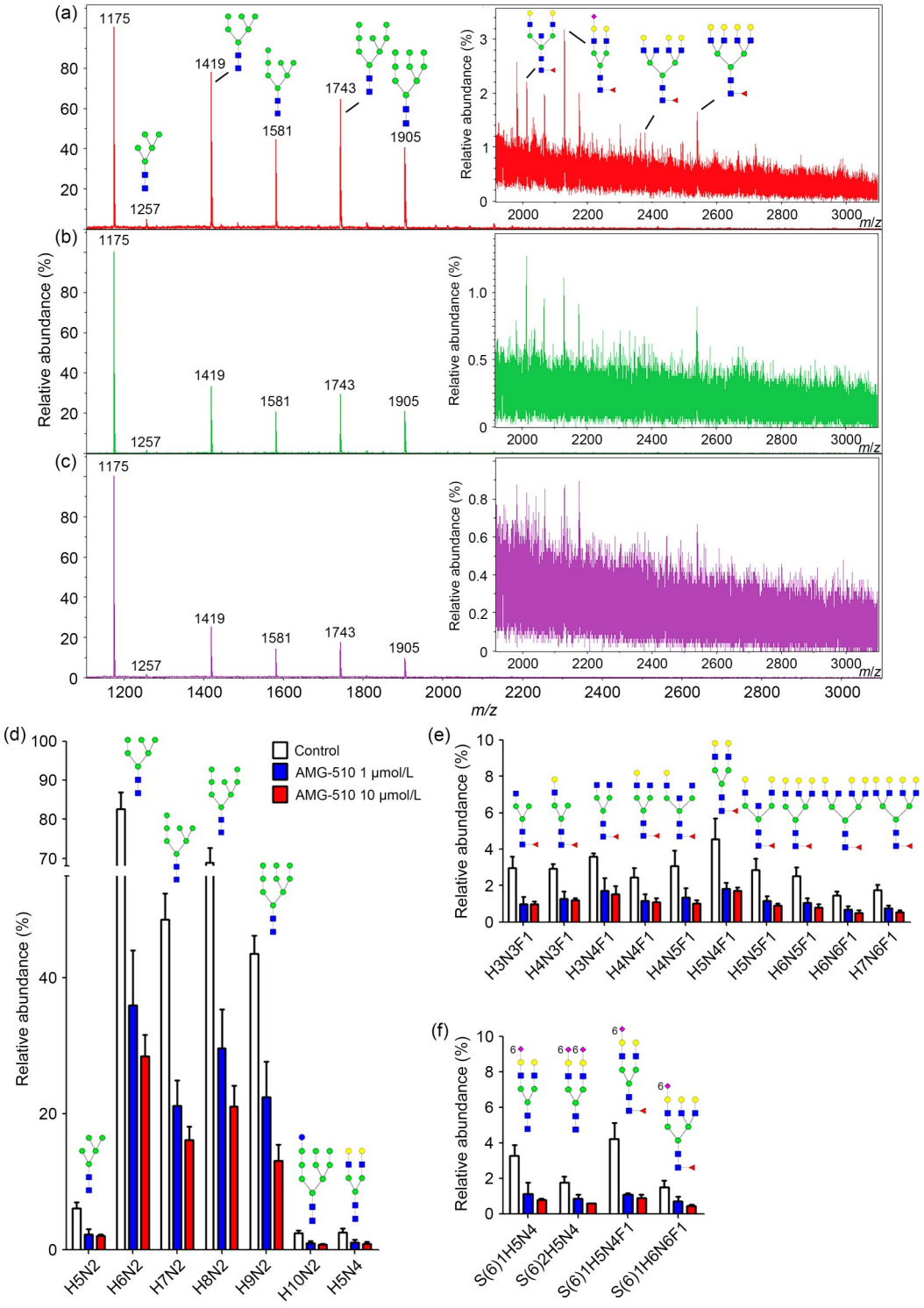

Fig. 3 Matrix-assisted laser desorption/ionization-mass spectrometry (MALDI-MS) spectra of *N*-glycans from the MIA PaCa-2 cell line and quantitative comparison of different types of *N*-glycans. (a) Untreated; (b) 1 μmol/L AMG-510; (c) 10 μmol/L AMG-510; (d) High-mannose and galactosylated *N*-glycans; (e) Fucosylated *N*-glycans; (f) Sialylated and/or fucosylated *N*-glycans.

Ctrl group (Figs. 4e–4h, Table S4). In the PDAC-D group, six *N*-glycans (H3N4F1, H4N4F1, H3N5F1, S(6)2H5N4, S(6)1H4N4F1, and S(6)1H5N4F1) were found to be significantly increased (Figs. 4f–4h), and

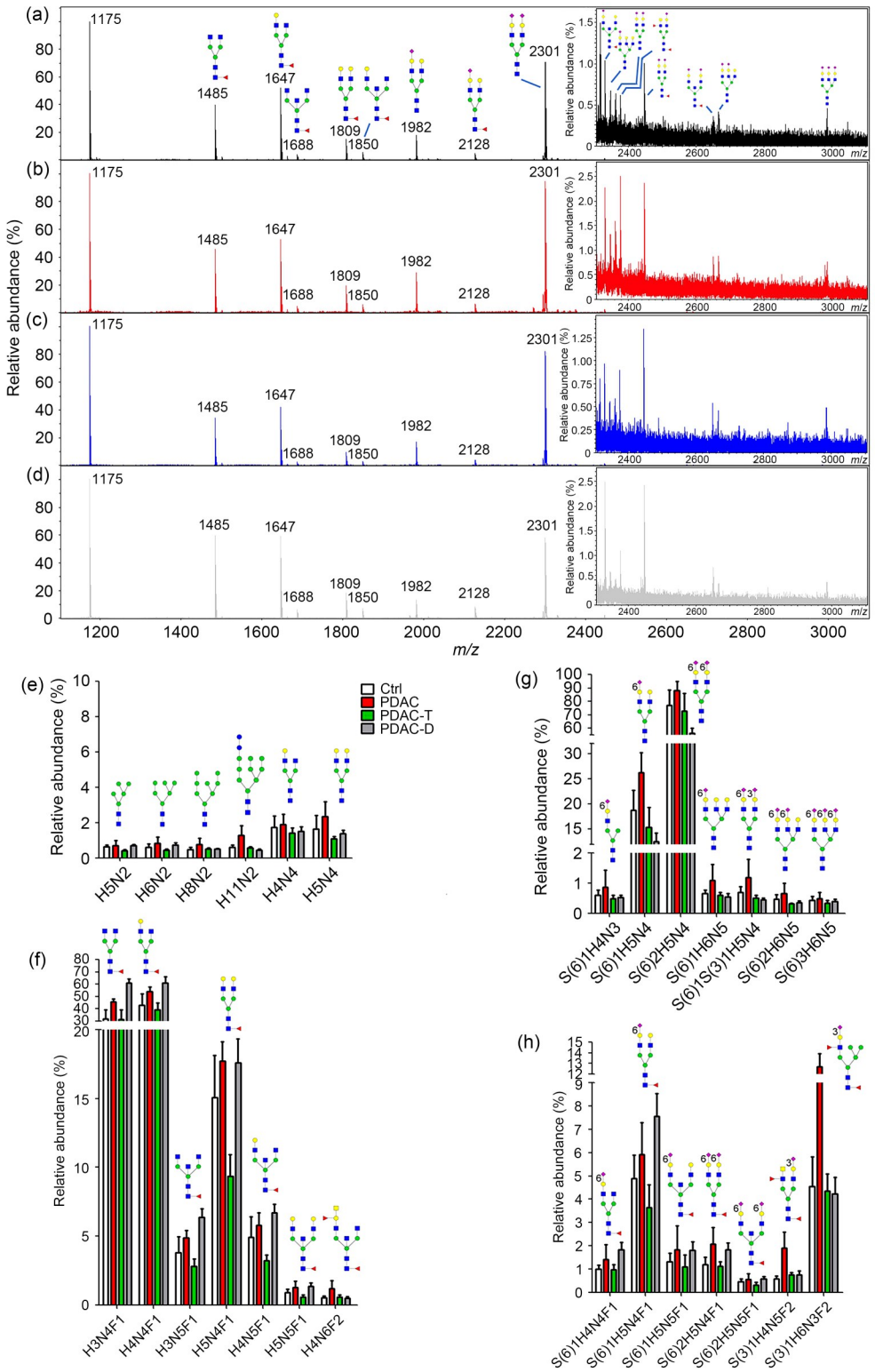

Fig. 4 Matrix-assisted laser desorption/ionization mass spectrometry (MALDI-MS) spectra of serum *N*-glycans and quantitative analysis of different types of *N*-glycans. (a) Healthy controls (Ctrl); (b) Untreated pancreatic ductal adenocarcinoma (PDAC) patients (PDAC); (c) PDAC patients with surgery and chemotherapy (PDAC-T); (d) Untreated PDAC patients with additional diseases (PDAC-D); (e) High-mannose and galactosylated *N*-glycans; (f) Fucosylated *N*-glycans; (g) Sialylated *N*-glycans; (h) Fucosylated and sialylated *N*-glycans.

only H3N4F1 was increased significantly in both the PDAC and PDAC-D groups compared with the Ctrl group. Apparently, other diseases affect different types of *N*-glycans, which may lead to false negative diagnosis in PDAC-D patients using *N*-glycan biomarkers identified in PDAC patients. Ideally, the PDAC-specific glycosylation biomarker should not be affected by other diseases.

We also found that surgery and chemotherapy had similar inhibitory effects on *N*-glycosylation observed in MIA PaCa-2 cells treated with AMG-510 (Figs. 4e–4h, Table S4). All *N*-glycans detected in PDAC sera were decreased in the PDAC-T group, and this decrease was mostly significant (Table S4). We believe that the general reduction in *N*-glycosylation in the PDAC-T sera is mainly due to the excision of tumors that actively secrete PDAC-associated *N*-glycoproteins into the circulation (Pan et al., 2014). Although the chemotherapy used in the PDAC-T group was not AMG-510, the antitumor properties of different chemicals may share the same mechanism of *N*-glycosylation inhibition, which indeed requires further investigation.

The analysis of global *N*-glycans did not reveal changes in PDAC patients similar to those in pancreatic cell lines. As aforementioned, many factors other than PDAC can affect the *N*-glycan levels in the blood. In addition, certain mechanisms exist to regulate the blood glycoprotein homeostasis (Lee et al., 2002; Roopenian and Akilesh, 2007), and plasma glycoproteins are also involved in homeostasis and thrombosis (Preston et al., 2013). Therefore, the exact PDAC-specific glycosylation changes should be unveiled by analyzing the detailed glycosylation information of specific glycoproteins (Vreeker et al., 2020), as the protein carriers of glycans are responsible for aberrant glycosylation-associated functional abnormalities under disease conditions.

3.4 *N*-Glycopeptide analysis of pancreatic cell lines and human sera

In order to determine the specific *N*-glycosylation changes in PDAC, *N*-glycopeptides from cell and serum samples were analyzed by LC-MS/MS. The glycosite-containing peptides were enriched by SPEG for the identification of corresponding *N*-glycoproteins. Among the three studied pancreatic cell lines, 267 *N*-glycoproteins were identified in hTERT-HPNE cells, 163 *N*-glycoproteins were identified in MIA PaCa-2 cells, and 264 *N*-glycoproteins were identified in AsPC-1 cells. The Venn diagram shows the number of unique and shared proteins in all cell lines (Fig. S3). The decreased amount of identified *N*-glycoprotein in MIA PaCa-2 cells compared with the other two cell lines may explain the previous results of overall *N*-glycan analysis. Although the number of *N*-glycoproteins in AsPC-1 was close to that in hTERT-HPNE, there were 93 unique *N*-glycoproteins identified only in AsPC-1. Thus, the overall changes in *N*-glycan levels in the three pancreatic cell lines should be attributed to shared and unique *N*-glycoproteins (Table S5). Consequently, the overall analysis of *N*-glycans will hardly provide accurate PDAC-specific biomarkers.

Next, we aimed to discover PDAC-specific *N*-glycosylation changes. *N*-Glycoproteins identified in human sera were first compared to *N*-glycoproteins in pancreatic cell lines to identify potential correlations between PDAC tumors and sera. A total of 45 proteins were shared by sera and one or more of the pancreatic cell lines (Table S6). Subsequently, intact *N*-glycopeptides from human sera (four groups) were enriched by HILIC for LC-MS/MS analysis. Therefore, the search for site-specific *N*-glycosylation information was focused on these 45 previously identified proteins. Based on the previous results of *N*-glycan analysis for the pancreatic cell lines and human sera, we propose that an ideal serum *N*-glycosylation biomarker for PDAC should possess the following criteria: (1) unique presence in PDAC compared with the Ctrl group; (2) unaffected in the PDAC-D group; (3) partially or fully reversed by clinical treatments.

According to the above criteria, two unique site-specific *N*-glycosylation changes were found in complement component 9 (C9) and α-2-HS-glycoprotein (AHSG). C9 is involved in complement activation, a defence mechanism against cancer (Afshar-Kharghan, 2017). Significantly increased levels of C9 and its fucosylation glycoforms were found in lung cancer sera (Narayanasamy et al., 2011); however, the relationship between C9 and PDAC has not been explored. Herein, we found a unique *N*-glycan (S(6)2H5N4F1) at the *N*-glycosite 415 of C9 in the PDAC group compared with the Ctrl group (Fig. 5). This *N*-glycan, along with the other types (S(6)1H5N4, S(6)2H5N4, and/or S(6)1S(3)1H5N4) found in the Ctrl group at

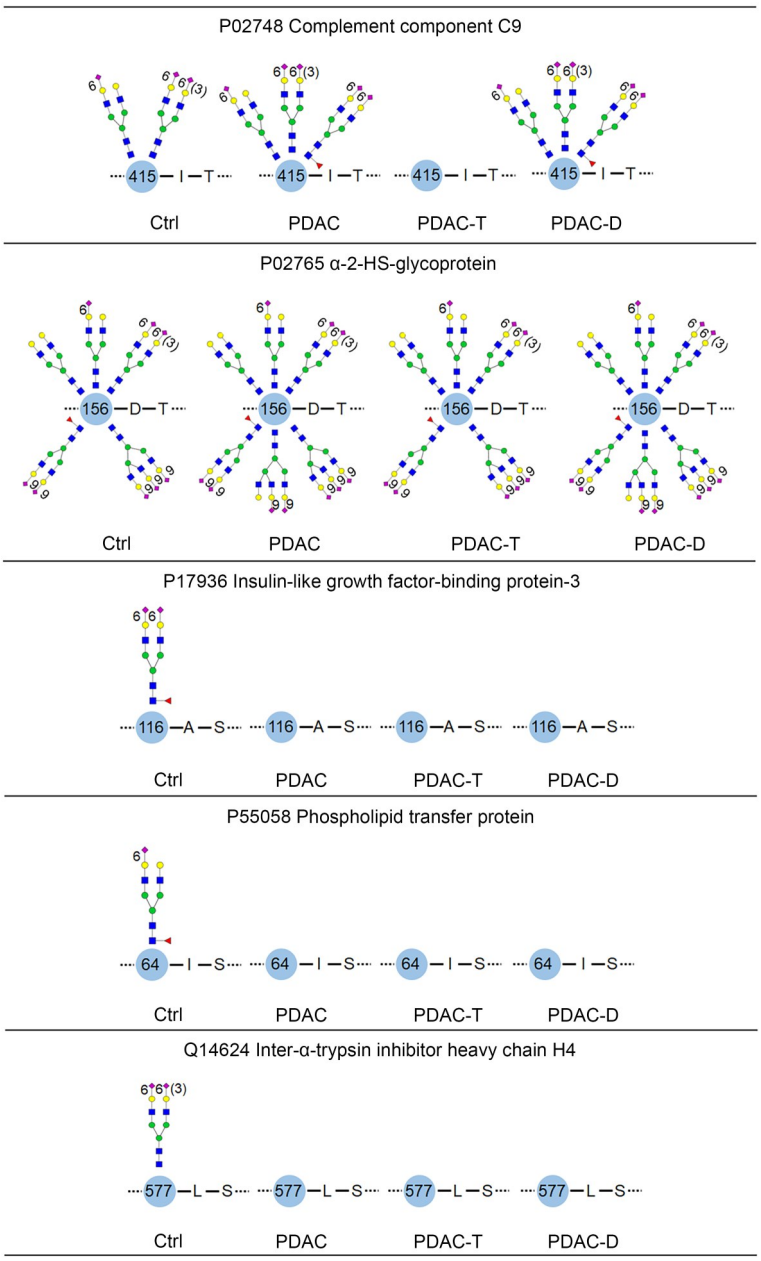

Fig. 5 Site-specific *N*-glycosylation changes in selected pancreatic ductal adenocarcinoma (PDAC)-specific proteins. The accession numbers, protein names, and *N*-glycosylation motifs of relevant glycoproteins are displayed. The numbers in the blue circles represent the position of asparagine on the protein sequence. Ctrl, healthy controls; PDAC, untreated PDAC patients; PDAC-T, PDAC patients with surgery and chemotherapy; PDAC-D, untreated PDAC patients with additional diseases.

N-glycosite 415, completely disappeared in the PDAC-T group. Importantly, no glycosylation change at *N*-glycosite 415 was observed between the PDAC and PDAC-D groups, indicating the specificity of this site-specific *N*-glycosylation change. ASHG has also been reported to be increased in the PDAC serum (Chen et al., 2013), but its *N*-glycosylation in PDAC was still unknown. In our work, a unique *N*-glycan (S(6)2H6N5) at the *N*-glycosite 156 of ASHG was discovered in the PDAC group compared with the Ctrl group (Fig. 5). Clinical treatments targeted only this unique *N*-glycosylation but no other types originally found in the Ctrl group. No change at the *N*-glycosite 156 was observed between the PDAC and PDAC-D groups; therefore, we propose that two unique *N*-glycosylation changes identified in C9 and

ASHG could serve as potential diagnostic and prognostic biomarkers.

In addition to increased *N*-glycosylation in PDAC, LC-MS/MS analysis revealed three *N*-glycosites from three proteins, of which unique glycosylation was only detected in the Ctrl group. Insulin-like growth factor-binding protein-3 (IGFBP-3) is a transporter protein for insulin-like growth factor that sensitizes chemo-resistant PDAC cells by activating apoptosis (Mofid et al., 2020). In a case-control study, the serum levels of IGFBP-3 were associated with an increased risk of PC mortality (Lin et al., 2004). We detected a unique glycan (S(6)2H5N4F1) only at the *N*-glycosite 116 of IGFBP-3 in the Ctrl group, while the same amino acid was not glycosylated in the other groups (Fig. 5). The roles of two other proteins, phospholipid transfer protein (PLTP) and inter-α-trypsin inhibitor heavy chain H4 (ITIH4), are unclear in PDAC. However, we also identified unique glycans in PLTP (S(6)1H5N4F1 at N64) and ITIH4 (S(6)2H5N4 and/or S(6)1S(3)1H5N4 at N577) (Fig. 5). The disappearance of the unique *N*-glycosylation in PDAC does not allow the monitoring of response to clinical treatment but still can serve as a potential diagnostic biomarker if used in conjugation with other markers in a panel.

4 Discussion

Unlike previous reports that analyzed only one type of biological samples (cells, tissues, or serum) (Zhao et al., 2007; Park et al., 2015; Lu et al., 2021), our study sought to investigate potential correlations among PDAC cells, clinical serum samples, and therapeutic treatments. To mimic the oncogenic process, a primary tumor cell line (MIA PaCa-2) and a metastatic tumor cell line (AsPC-1) were used. The results of *N*-glycan analysis demonstrated that contrasting changes in *N*-glycosylation had already occurred in primary tumor cells, suggesting that early detection of PDAC-specific *N*-glycosylation could facilitate clinical diagnosis. Meanwhile, the FDA-approved AMG-510 targeting *KRAS* G12C could significantly inhibit *N*-glycosylation levels in MIA PaCa-2 cells. Based on these results, early diagnosis and monitoring of treatment response by detecting *N*-glycosylation changes in clinical samples (such as serum) seemed a possibility. However, we found that the *N*-glycosylation status in the serum was different from that in the cell lines. Glycosylation in blood circulation can be affected by different disease conditions, with CA19-9 being an example. Therefore, the discovery of PDAC-specific *N*-glycosylation biomarkers is not an easy task. The overall analysis of *N*-glycans failed to reveal the same contrasting changes in different cell lines. Since glycosylation regulates protein structures and functions (Esmail and Manolson, 2021), identifying the exact changes in glycoforms on PDAC-associated proteins is imperative. In our work, *N*-glycoproteins shared by cell lines and human sera were selected for the analysis of intact glycopeptides. An important aspect of intact glycopeptide analysis in our work was to monitor the effects of treatment and other disease conditions on the *N*-glycosylation changes identified in PDAC serum. A biomarker affected by other disease conditions cannot be used to specifically diagnose a particular disease. As the mean age of PDAC patients enrolled in our study was over 60 years, these patients commonly had other diseases; *N*-glycosylation changes affected by diseases other than PDAC may lead to false-negative diagnosis in future clinical applications. Meanwhile, clinical treatments should theoretically reverse the aberrant glycosylation of the PDAC-specific biomarker in question. Consequently, the two unique *N*-glycoforms identified in C9 and AHSG are promising candidates for validating their roles as diagnostic and prognostic biomarkers. In addition, the disappearance of unique glycosylation in PDAC can also indicate a disease status. Additionally, our methods can be used to study the glycosylation of tumor immune checkpoints, such as cytotoxic T-lymphocyte-associated antigen-4 (CTLA-4) and programmed cell death protein-1 (PD-1), as these proteins are highly glycosylated (Gao et al., 2022).

Due to the limited number of clinical samples in our study, we were unable to separately evaluate the effects of surgery and chemotherapy on PDAC-specific glycosylation. Besides, the heterogeneity of glycosylation changes among individual patients is unknown. To study the *N*-glycosylation changes during PDAC development, we are currently expanding the number of PDAC patients recruited to include more clinical information on disease stages. The specificity and sensitivity of selected glycosylation biomarkers in this work will be investigated individually or in cohorts in subsequent work.

5 Conclusions

In the current study, *N*-glycan analysis revealed contrasting changes in PDAC cell lines, which could be significantly inhibited by AMG-510 treatment. The correlation between cell lines and human serum was investigated by focusing on *N*-glycoproteins shared by PDAC cell lines and serum samples. Intact *N*-glycopeptides from 45 shared *N*-glycoproteins were assessed by LC-MS/MS, which yielded two PDAC-unique and three Ctrl-unique *N*-glycoforms. Statistical analysis indicated that in metastatic AsPC-1 cells, glycosylation was restored to a level similar to that of hTERT-HPNE, suggesting a potential feedback regulation of glycosylation during the metastatic stage of PDAC carcinogenesis. We also found that surgery and chemotherapy had similar inhibitory effects on *N*-glycosylation in MIA PaCa-2 cells treated with AMG-510. PDAC serum analysis suggested that the general decrease in *N*-glycosylation in PDAC-T serum was primarily due to the excision of tumors that actively secretes PDAC-associated *N*-glycoproteins into the circulation. With regard to tumor marker selection, we suggest that ideal PDAC serum *N*-glycosylation biomarkers should comply with the following criteria: (1) uniqueness in PDAC compared to the Ctrl group; (2) the PDAC-D group is unaffected; (3) changes are partially or completely reversed by clinical treatment. We believe that the site-specific *N*-glycosylation changes (used individually or in a panel) identified in this study have the potential to be developed into clinical diagnostic and/or prognostic biomarkers.

Data availability statement

All data generated or analyzed during this study are included in this published article and its supplementary information files.

Acknowledgments

This work was supported by the Soochow University Start-up Fund, the Priority Academic Program Development of the Jiangsu Higher Education Institutes (PAPD), the Jiangsu Science and Technology Plan Funding (No. BX2022023), the Jiangsu Shuangchuang Boshi Funding (No. JSSCBS20210697), and the Foundation of Zhejiang Provincial Administration of Traditional Chinese Medicine (No. 2020ZB020), China.

Author contributions

Mingming XU, Zhaoliang LIU, Wenhua HU, and Shuang YANG contributed to data collection, analysis, interpretation, and writing of the manuscript. Sufeng CHEN, Peng XIA, and Jing DU contributed to sample collection. Ying HAN and Zhen WU contributed to mass spectrometry study. Mingming XU, Xumin ZHANG, Piliang HAO, Jun XIA, and Shuang YANG contributed to the study concept and design, study supervision, and critical revision of the manuscript. All authors have read and approved the final manuscript, and therefore, have full access to all the data in the study and take responsibility for the integrity and security of the data.

Compliance with ethics guidelines

Mingming XU, Zhaoliang LIU, Wenhua HU, Ying HAN, Zhen WU, Sufeng CHEN, Peng XIA, Jing DU, Xumin ZHANG, Piliang HAO, Jun XIA, and Shuang YANG declare no competing interests.

This study was approved by the Research Ethics Committees of Zhejiang Provincial People's Hospital (No. QT2022387). The written informed consent was provided to patients in advance.

References

Abd-El-Halim YM, el Kaoutari A, Silvy F, et al., 2021. A glycosyltransferase gene signature to detect pancreatic ductal adenocarcinoma patients with poor prognosis. *eBioMedicine*, 71:103541. https://doi.org/10.1016/j.ebiom.2021.103541

Afshar-Kharghan V, 2017. The role of the complement system in cancer. *J Clin Invest*, 127(3):780-789. https://doi.org/10.1172/jci90962

Ardito CM, Grüner BM, Takeuchi KK, et al., 2012. EGF receptor is required for KRAS-induced pancreatic tumorigenesis. *Cancer Cell*, 22(3):304-317. https://doi.org/10.1016/j.ccr.2012.07.024

Bassagañas S, Carvalho S, Dias AM, et al., 2014. Pancreatic cancer cell glycosylation regulates cell adhesion and invasion through the modulation of α2β1 integrin and E-cadherin function. *PLoS ONE*, 9(5):e98595. https://doi.org/10.1371/journal.pone.0098595

Canon J, Rex K, Saiki AY, et al., 2019. The clinical KRAS (G12C) inhibitor AMG 510 drives anti-tumour immunity. *Nature*, 575(7781):217-223. https://doi.org/10.1038/s41586-019-1694-1

Cao LW, Lih TM, Hu YW, et al., 2022. Characterization of core fucosylation via sequential enzymatic treatments of intact glycopeptides and mass spectrometry analysis. *Nat Commun*, 13:3910. https://doi.org/10.1038/s41467-022-31472-4

Ceroni A, Maass K, Geyer H, et al., 2008. GlycoWorkbench: a tool for the computer-assisted annotation of mass spectra of glycans. *J Proteome Res*, 7(4):1650-1659. https://doi.org/10.1021/pr7008252

Chen HH, Deng ZA, Huang CC, et al., 2017. Mass spectrometric profiling reveals association of *N*-glycan patterns with epithelial ovarian cancer progression. *Tumour Biol*, 39(7):1010428317716249.

https://doi.org/10.1177/1010428317716249

Chen J, Wu W, Chen LJ, et al., 2013. Profiling the potential tumor markers of pancreatic ductal adenocarcinoma using 2D-DIGE and MALDI-TOF-MS: up-regulation of Complement C3 and alpha-2-HS-glycoprotein. *Pancreatology*, 13(3):290-297. https://doi.org/10.1016/j.pan.2013.03.010

de Leoz MLA, Young LJT, An HJ, et al., 2011. High-mannose glycans are elevated during breast cancer progression. *Mol Cell Proteomics*, 10(1):M110.002717. https://doi.org/10.1074/mcp.M110.002717

Esmail S, Manolson MF, 2021. Advances in understanding *N*-glycosylation structure, function, and regulation in health and disease. *Eur J Cell Biol*, 100(7-8):151186. https://doi.org/10.1016/j.ejcb.2021.151186

Gao ZR, Ling XY, Shi CY, et al., 2022. Tumor immune checkpoints and their associated inhibitors. *J Zhejiang Univ-Sci B (Biomed & Biotechnol)*, 23(10):823-843. https://doi.org/10.1631/jzus.B2200195

Gold G, Goh SK, Christophi C, et al., 2019. Dilemmas and limitations interpreting carbohydrate antigen 19-9 elevation after curative pancreatic surgery: a case report. *Int J Surg Case Rep*, 54:20-22. https://doi.org/10.1016/j.ijscr.2018.11.022

Holst S, Belo AI, Giovannetti E, et al., 2017. Profiling of different pancreatic cancer cells used as models for metastatic behaviour shows large variation in their *N*-glycosylation. *Sci Rep*, 7:16623. https://doi.org/10.1038/s41598-017-16811-6

Hruban RH, Petersen GM, Ha PK, et al., 1998. Genetics of pancreatic cancer: from genes to families. *Surg Oncol Clin North Am*, 7(1):1-23. https://doi.org/10.1016/S1055-3207(18)30282-5

Hu HF, Ye Z, Qin Y, et al., 2021. Mutations in key driver genes of pancreatic cancer: molecularly targeted therapies and other clinical implications. *Acta Pharmacol Sin*, 42(11):1725-1741. https://doi.org/10.1038/s41401-020-00584-2

Lee SJ, Evers S, Roeder D, et al., 2002. Mannose receptor-mediated regulation of serum glycoprotein homeostasis. *Science*, 295(5561):1898-1901. https://doi.org/10.1126/science.1069540

Levink IJM, Klatte DCF, Hanna-Sawires RG, et al., 2022. Longitudinal changes of serum protein N-Glycan levels for earlier detection of pancreatic cancer in high-risk individuals. *Pancreatology*, 22(4):497-506. https://doi.org/10.1016/j.pan.2022.03.021

Liang Y, Wang W, Fang C, et al., 2016. Clinical significance and diagnostic value of serum CEA, CA19-9 and CA72-4 in patients with gastric cancer. *Oncotarget*, 7(31):49565-49573. https://doi.org/10.18632/oncotarget.10391

Lin YS, Tamakoshi A, Kikuchi S, et al., 2004. Serum insulin-like growth factor-I, insulin-like growth factor binding protein-3, and the risk of pancreatic cancer death. *Int J Cancer*, 110(4):584-588. https://doi.org/10.1002/ijc.20147

Liu LY, Zhu B, Fang Z, et al., 2021. Automated intact glycopeptide enrichment method facilitating highly reproducible analysis of serum site-specific N-glycoproteome. *Anal Chem*, 93(20):7473-7480. https://doi.org/10.1021/acs.analchem.1c00645

Lu HR, Xiao KJ, Tian ZX, 2021. Benchmark of site- and structure-specific quantitative tissue N-glycoproteomics for discovery of potential N-glycoprotein markers: a case study of pancreatic cancer. *Glycoconj J*, 38(2):213-231. https://doi.org/10.1007/s10719-021-09994-8

Lumibao JC, Tremblay JR, Hsu J, et al., 2022. Altered glycosylation in pancreatic cancer and beyond. *J Exp Med*, 219(6):e20211505. https://doi.org/10.1084/jem.20211505

Marrelli D, Caruso S, Pedrazzani C, et al., 2009. CA19-9 serum levels in obstructive jaundice: clinical value in benign and malignant conditions. *Am J Surg*, 198(3):333-339. https://doi.org/10.1016/j.amjsurg.2008.12.031

Maxwell E, Tan Y, Tan YX, et al., 2012. GlycReSoft: a software package for automated recognition of glycans from LC/MS data. *PLoS ONE*, 7(9):e45474. https://doi.org/10.1371/journal.pone.0045474

Mofid MR, Gheysarzadeh A, Bakhtiyari S, 2020. Insulin-like growth factor binding protein 3 chemosensitizes pancreatic ductal adenocarcinoma through its death receptor. *Pancreatology*, 20(7):1442-1450. https://doi.org/10.1016/j.pan.2020.07.406

Munkley J, 2019. The glycosylation landscape of pancreatic cancer (Review). *Oncol Lett*, 17(3):2569-2575. https://doi.org/10.3892/ol.2019.9885

Narayanasamy A, Ahn JM, Sung HJ, et al., 2011. Fucosylated glycoproteomic approach to identify a complement component 9 associated with squamous cell lung cancer (SQLC). *J Proteomics*, 74(12):2948-2958. https://doi.org/10.1016/j.jprot.2011.07.019

Nie S, Lo A, Wu J, et al., 2014. Glycoprotein biomarker panel for pancreatic cancer discovered by quantitative proteomics analysis. *J Proteome Res*, 13(4):1873-1884. https://doi.org/10.1021/pr400967x

Pan S, Tamura Y, Chen R, et al., 2012. Large-scale quantitative glycoproteomics analysis of site-specific glycosylation occupancy. *Mol Biosyst*, 8(11):2850-2856. https://doi.org/10.1039/c2mb25268f

Pan S, Chen R, Tamura Y, et al., 2014. Quantitative glycoproteomics analysis reveals changes in N-glycosylation level associated with pancreatic ductal adenocarcinoma. *J Proteome Res*, 13(3):1293-1306. https://doi.org/10.1021/pr4010184

Park HM, Hwang MP, Kim YW, et al., 2015. Mass spectrometry-based N-linked glycomic profiling as a means for tracking pancreatic cancer metastasis. *Carbohydr Res*, 413:5-11. https://doi.org/10.1016/j.carres.2015.04.019

Preston RJS, Rawley O, Gleeson EM, et al., 2013. Elucidating the role of carbohydrate determinants in regulating hemostasis: insights and opportunities. *Blood*, 121(19):3801-3810. https://doi.org/10.1182/blood-2012-10-415000

Reily C, Stewart TJ, Renfrow MB, et al., 2019. Glycosylation in health and disease. *Nat Rev Nephrol*, 15(6):346-366. https://doi.org/10.1038/s41581-019-0129-4

Rho JH, Mead JR, Wright WS, et al., 2014. Discovery of sialyl Lewis A and Lewis X modified protein cancer biomarkers using high density antibody arrays. *J Proteomics*, 96:291-299. https://doi.org/10.1016/j.jprot.2013.10.030

Roopenian DC, Akilesh S, 2007. FcRn: the neonatal Fc receptor comes of age. *Nat Rev Immunol*, 7(9):715-725. https://doi.org/10.1038/nri2155

Ryan DP, Hong TS, Bardeesy N, 2014. Pancreatic adenocarcinoma. *N Engl J Med*, 371(11):1039-1049. https://doi.org/10.1056/NEJMra1404198

Sato Y, Fujimoto D, Uehara K, et al., 2016. The prognostic value of serum CA 19-9 for patients with advanced lung adenocarcinoma. *BMC Cancer*, 16:890. https://doi.org/10.1186/s12885-016-2897-6

Sethi MK, Hancock WS, Fanayan S, 2016. Identifying *N*-glycan biomarkers in colorectal cancer by mass spectrometry. *Acc Chem Res*, 49(10):2099-2106. https://doi.org/10.1021/acs.accounts.6b00193

Sung H, Ferlay J, Siegel RL, et al., 2021. Global Cancer Statistics 2020: GLOBOCAN estimates of incidence and mortality worldwide for 36 cancers in 185 countries. *CA Cancer J Clin*, 71(3):209-249. https://doi.org/10.3322/caac.21660

Talar-Wojnarowska R, Gasiorowska A, Olakowski M, et al., 2011. Clinical value of serum neopterin, tissue polypeptide-specific antigen and CA19-9 levels in differential diagnosis between pancreatic cancer and chronic pancreatitis. *Pancreatology*, 10(6):689-694. https://doi.org/10.1159/000320693

Taparra K, Wang HL, Malek R, et al., 2018. O-GlcNAcylation is required for mutant *KRAS*-induced lung tumorigenesis. *J Clin Invest*, 128(11):4924-4937. https://doi.org/10.1172/JCI94844

Vreeker GCM, Hanna-Sawires RG, Mohammed Y, et al., 2020. Serum *N*-Glycome analysis reveals pancreatic cancer disease signatures. *Cancer Med*, 9(22):8519-8529. https://doi.org/10.1002/cam4.3439

Vukobrat-Bijedic Z, Husic-Selimovic A, Sofic A, et al., 2013. Cancer antigens (CEA and CA 19-9) as markers of advanced stage of colorectal carcinoma. *Med Arch*, 67(6):397-401. https://doi.org/10.5455/medarh.2013.67.397-401

Xiao HP, Sun FX, Suttapitugsakul S, et al., 2019. Global and site-specific analysis of protein glycosylation in complex biological systems with Mass Spectrometry. *Mass Spectrom Rev*, 38(4-5):356-379. https://doi.org/10.1002/mas.21586

Xu MM, Hu WH, Liu ZL, et al., 2021. Glycoproteomic bioanalysis of exosomes by LC−MS for early diagnosis of pancreatic cancer. *Bioanalysis*, 13(11):861-864. https://doi.org/10.4155/bio-2021-0036

Xu MM, Jin H, Wu Z, et al., 2022. Mass spectrometry-based analysis of serum N-glycosylation changes in patients with Parkinson's disease. *ACS Chem Neurosci*, 13(12):1719-1726. https://doi.org/10.1021/acschemneuro.2c00264

Yang S, Li Y, Shah P, et al., 2013. Glycomic analysis using glycoprotein immobilization for glycan extraction. *Anal Chem*, 85(11):5555-5561. https://doi.org/10.1021/ac400761e

Yang S, Jankowska E, Kosikova M, et al., 2017. Solid-phase chemical modification for sialic acid linkage analysis: application to glycoproteins of host cells used in influenza virus propagation. *Anal Chem*, 89(17):9508-9517. https://doi.org/10.1021/acs.analchem.7b02514

Yang S, Wu WW, Shen RF, et al., 2018. Identification of sialic acid linkages on intact glycopeptides via differential chemical modification using intactGIG-HILIC. *J Am Soc Mass Spectrom*, 29(6):1273-1283. https://doi.org/10.1007/s13361-018-1931-0

Yang S, Xia J, Yang ZR, et al., 2021. Lung cancer molecular mutations and abnormal glycosylation as biomarkers for early diagnosis. *Cancer Treat Res Commun*, 27:100311. https://doi.org/10.1016/j.ctarc.2021.100311

Zhang H, Li XJ, Martin DB, et al., 2003. Identification and quantification of N-linked glycoproteins using hydrazide chemistry, stable isotope labeling and mass spectrometry. *Nat Biotechnol*, 21(6):660-666. https://doi.org/10.1038/nbt827

Zhang W, Wang YY, Dong X, et al., 2021. Elevated serum CA19-9 indicates severe liver inflammation and worse survival after curative resection in hepatitis B-related hepatocellular carcinoma. *Biosci Trends*, 15(6):397-405. https://doi.org/10.5582/bst.2021.01517

Zhao J, Qiu WL, Simeone DM, et al., 2007. *N*-linked glycosylation profiling of pancreatic cancer serum using capillary liquid phase separation coupled with mass spectrometric analysis. *J Proteome Res*, 6(3):1126-1138. https://doi.org/10.1021/pr0604458

Supplementary information

Materials and methods; Tables S1–S6; Figs. S1–S3